UNIVERSITY OF CALIFORNIA, SAN DIEGO

Engineered proteins with activating module for reprogramming of cell signaling pathway

A Thesis submitted in partial satisfaction of the

requirements for the degree

Master of Science

in

Bioengineering

by

Lunan Shao

Committee in Charge:

Professor Yingxiao Wang, Chair
Professor Adam J. Engler
Professor Xiaohua Huang

2017

Signature Page

The Thesis of Lunan Shao is approved, and it is acceptable in quality and form for publication on microfilm and electronically:

Chair

University of California, San Diego

2017

Table of Contents

List of Figures

Acknowledgements

I would like to acknowledge Dr. Yingxiao Wang for his invaluable guidance and support as the chair of my committee. Also, I would like to acknowledge Dr. Hsin-Hung Lin and Pengzhi Wang, who have worked with me and helped me a lot along the way of this project.

Abstract of the Thesis

Engineered proteins with activating module for reprogramming of cell signaling pathway

by

Lunan Shao

Master of Science in Bioengineering

University of California, San Diego, 2017

Professor Yingxiao Wang, Chair

Programmed cell death protein 1 (PD-1) and signal regulatory protein α (SIRPα) are receptors that transduce inhibitory signals to negatively regulate effector functions of immune cells, which were both utilized by cancers to evade and inhibit the immune response. Through protein engineering, integrated sensing and activating proteins (iSNAPs) were developed to replace the cytoplasmic domains of PD-1 and SIRPα

receptors. With Fyn as the activating module, engineered Fyn-iSNAP replaced the cytoplasmic tail of PD-1, which was intended to reprogram PD-1/PD-L1 inhibitory signaling into activating Fyn signaling upon ligand binding. However, characterization of Fyn-iSNAP in HeLa cells demonstrated that this engineered protein failed to show desired functions. In the second chapter, in order to rewire SIRPα/CD47 inhibitory pathway, Shp2-iSNAPs and Syk-iSNAPs were developed and used to replace the original SIRPα cytoplasmic domain in our previous studies (data not published yet). In order to increase gene delivery efficiency, the sizes of the engineered SIRPα-iSNAPs were reduced. The expression of the truncated proteins in mouse macrophages led to enhanced phagocytosis of opsonized red blood cells (RBCs). Also, human promyelocytic leukemia cell derived macrophages (PLDMs) were engineered for the first time using the SIRPα-Shp2-iSNAPs and its truncated version, which demonstrated enhanced engulfment against opsonized RBCs as well as tumor cells. Therefore, these engineered proteins with activating module potentially offer a new approach for future cancer immunotherapy.

Chapter 1: The reprogramming of PD-1/PD-L1 inhibitory pathway in T cell with Fyn-iSNAPs

1.1 Background

1.1.1 T-cell activation

T-cell activation through T-cell antigen receptor (TCR) is important for effective acquired immune response to counteract the invasion of various pathogens. Upon TCR engagement with antigen peptides, Src family kinases, Lck and Fyn, are activated, leading to phosphorylation of CD3 molecules within the TCR complex [1,2]. Subsequently, doubly phosphorylated CD3ζ serves as a docking site for Syk family kinase ZAP-70, which leads to activation of ZAP-70 catalytic activity and its autophosphorylation [3]. Activated ZAP-70 phosphorylates downstream signaling molecules, such as LAT, which can potentially lead to T-cell activation [3,4]

In order to prevent immune hyperactivation and autoimmunity, T-cell activation involves the balance between activating and inhibiting signal [5]. In activated T cell, programmed cell death protein 1 (PD-1) is a receptor protein that is transcriptionally induced to negatively regulate T-cell activation [6]. PD-1 receptor is a 55 kDa transmembrane protein with its extracellular domain consisted of a single Ig-like variable domain, and its cytoplasmic domain encodes both immunoreceptor tyrosine-based inhibitory motif (ITIM) and an immunoreceptor tyrosine-based switch motif (ITSM) [7,8]. PD-1 receptor has two ligands, PD-1 ligand 1 (PD-L1) and PD-1 ligand 2 (PD-L2), and the receptor does not have enzymatic activity, but its cytoplasmic domain is the binding site for downstream proteins [9,10]. Upon ligand engagement, PD-1 is phosphorylated on tyrosine sites within ITIM and ITSM, which bind phosphatase SHP-2

that downregulates T cell activation by dephosphorylating CD3ζ chain in TCR and preventing recruitment of protein kinase ZAP70 [9].

1.1.2 Fyn kinase structure

T-cell activation is mediated through signaling cascades that transduce extracellular signals to intracellular responses, which lead to the effector functions of T cell. Activation of Fyn is closely involved with these signaling cascades by inducing binding of downstream signaling molecules, such as phosphatidylinositol 3-kinase (PI3K) and adhesion and degranulation-promoting adaptor protein (ADAP) [11,12]. Recruitment of these substrates through Src-homology (SH) domains allows Fyn to initiate and regulate diverse lymphocyte effector functions.

Fyn is 59 kDa non-receptor tyrosine kinase that has four Src-homology (SH) domains: the N-terminal SH4 domain, SH3 domain, SH2 domain and a tyrosine kinase domain (SH1) [13]. The SH4 domain contains a unique region that has two Cys residues, which contribute to Fyn functions [14]. The SH3 domain is consisted by a β-barrel structure that serves as a binding site for proline-rich peptide, and the SH2 domain specifically interacts with phosphorylated tyrosine sites [15]. The SH3 and SH2 domains help mediate the interaction between Fyn and its downstream substrates during phosphorylation [15].

Intramolecular interactions among SH domains determine Fyn conformation, which regulates Fyn activity by preventing excess kinase activation. At inactive state of Fyn, the SH2 domain binds to a phosphorylated regulatory tyrosine site (Tyr^{531}) at C-terminus, which results in occlusion of the kinase domain by the SH2 and SH3 domains. [16-18]. By dephosphorylating Tyr^{531} or removing this regulatory interaction by

competition from another more specific interacting ligand, the SH2 domain disassociates from the C-terminus, which exposes the SH1 domain, Fyn kinase becomes active to phosphorylate downstream proteins [19].

Based on the aforementioned function and structure of Fyn, an engineered protein with Fyn kinase as the activating module was developed to replace the original cytoplasmic tail of PD-1 receptor, which was intended to rewire the PD-1/PD-L1 inhibitory signaling pathway in T cells into an activating one and prevent cancer cells from evading the immune response.

1.2 Results

1.2.1 Development of Fyn-iSNAPs

To reprogram the downstream signal of PD-1 receptor, the ITIM and ITSM domain of PD-1 receptor was replaced by our engineered protein consisted of an interacting ligand of Fyn SH2/SH3 domain, fluorescence proteins, and full-length Fyn kinase. One of the interacting ligands, L1, in this engineered protein has high affinity of binding to Fyn SH2 domain, which was originally found in the hamster middle-sized tumor (HmT) antigen [20]. Another ligand, L2, adds a proline-rich region to the N-terminus of L1, which facilitates the additional binding of the SH3 domain in the purpose of further exposing the SH1 domain and activating Fyn kinase. Also, ITAM region from CD3ζ1 of TCR was used as one of the ligands, Z1. Even though this ITAM region has two tyrosine sites, it has low binding affinity to Fyn SH2 domain [21]. In addition, a control group with no ligand region was designed and named as control-Fyn-iSNAP (C-Fyn-iSNAP). The ligand regions are followed by cyan fluorescent protein, ECFP and yellow fluorescent protein, YPet, which can engage in FRET. In previous literature, FRET-based biosensors have been developed to visualize molecular dynamics in live cells [22]. When two fluorophores are apart, exciting ECFP with 433 nm light allows it to emit 476 nm light. However, when ECFP is in close proximity with YPet, the emitting light of ECFP is capable of exciting YPet, which results in YPet emitting 530 nm light. Following the FRET fluorescence protein pair, it is full-length Fyn kinase with SH domains and C-terminus protein sequence intact so that the structure and functions of the kinase are largely preserved. Therefore, upon PD-L1 engagement, the ligand in Fyn-iSNAP gets phosphorylated, and this phosphorylated tyrosine site competes with C-

terminal phosphorylated Tyr^{531} for binding to the SH2 domain. Then, it leads to the activation of Fyn kinase by exposing SH1 domain and an overall conformational change, which brings ECFP and YPet in proximity and results in a FRET/ECFP emission ratio change (Figure 1). Thus, when this engineered protein is utilized to replace original cytoplasmic domain of PD-1 receptor, it can both help visualize phosphorylation event at PD-1 cytoplasmic tail and, at the same time, transduce activating signals that lead to effector functions of T cell.

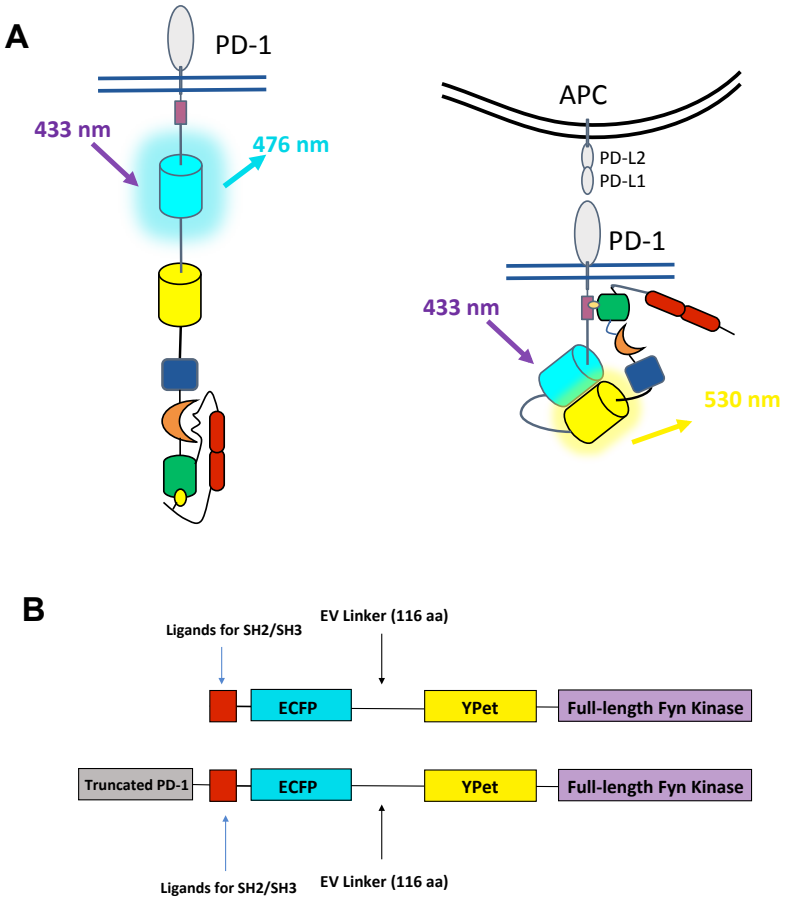

Figure 1: The structure and activation of the Fyn-iSNAP. (A) Schematic drawing of the Fyn-iSNAP and its intended activation mechanism upon PD-L1 engagement. (B) Schematic representation of the Fyn-iSNAP before and after being fused to the truncated PD-1 receptor.

1.2.2 Characterization of Fyn-iSNAPs in live mammalian cells

Fyn-iSNAPs with different ligands as well as a positive control, Z1-ZAP70-iSNAP (Z1-ZAP70-iSNAP), were transfected into a mammalian cell line, HeLa. Z1-ZAP70-iSNAP fused with truncated PD-1 reeptor was capable of sensing phosphorylation event (data not published yet). Pervanadate (PVD) was used to inhibit phosphatase activity within the cells, which increased the level of cellular tyrosine phosphorylation [23]. Therefore, PVD treatment can phosphorylate the tyrosine site

within the interacting ligands. As shown in Figure 2 and Figure 3, compared to Z1-Fyn-iSNAP, C-Fyn-iSNAP and the positive control, the cells transfected with L1-Fyn-iSNAP and L2-Fyn-iSNAP demonstrated relatively high basal level of FRET/ECFP emission ratio before PVD treatment. After adding PVD, all Fyn-iSNAPs showed no significant change in FRET/ECFP ratio when Z1-ZAP70-BA showed more than threefold FRET ratio change within 30 minutes. Also, for this positive control group, the change began between 5-10 minutes after stimulation.

Even though the cells were plated on glass bottom dish (Cell E&G) coated with the same concentration of fibronectin (Sigma), the cells transfected with L1-Fyn-iSNAP and L2-Fyn-iSNAP had different morphology compared to the other groups. Most L1- and L2-Fyn-iSNAPs transfected cells were flat and elongated, while those transfected with Z1-ZAP70-iSNAP, C-Fyn-iSNAP and Z1-Fyn-iSNAP retained their epithelial-like shape as shown in Figure 3.

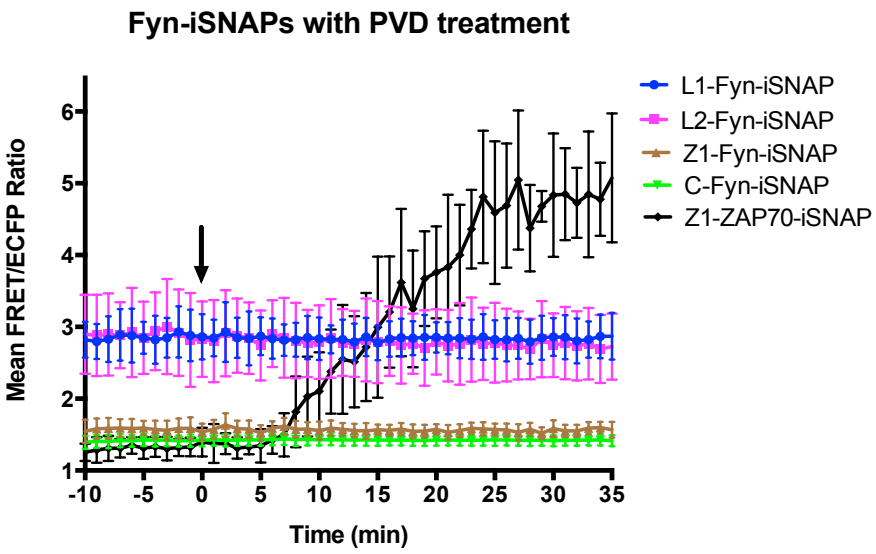

Figure 2: The normalized emission ratio time courses of Fyn-iSNAPs in response to pervanadate (PVD) treatment in HeLa cells. The time courses of normalized average FRET/ECFP ratios of L1-Fyn-iSNAP-Z1 (blue solid circles, n = 10), L2-Fyn-iSNAP (magenta squares, n = 10), Z1-Fyn-iSNAP (brown solid triangles, n = 10), C-Fyn-iSNAP (green solid triangles, n = 10) and positive control group: Z1-ZAP70-iSNAP (black triangles, n = 5) in HeLa cells before and after 20 μM PVD treatment (Arrow at 0 min indicates treatment time). The error bars represent the standard error of the mean (S.E.M.). Data are showed as mean ± S.E.M..

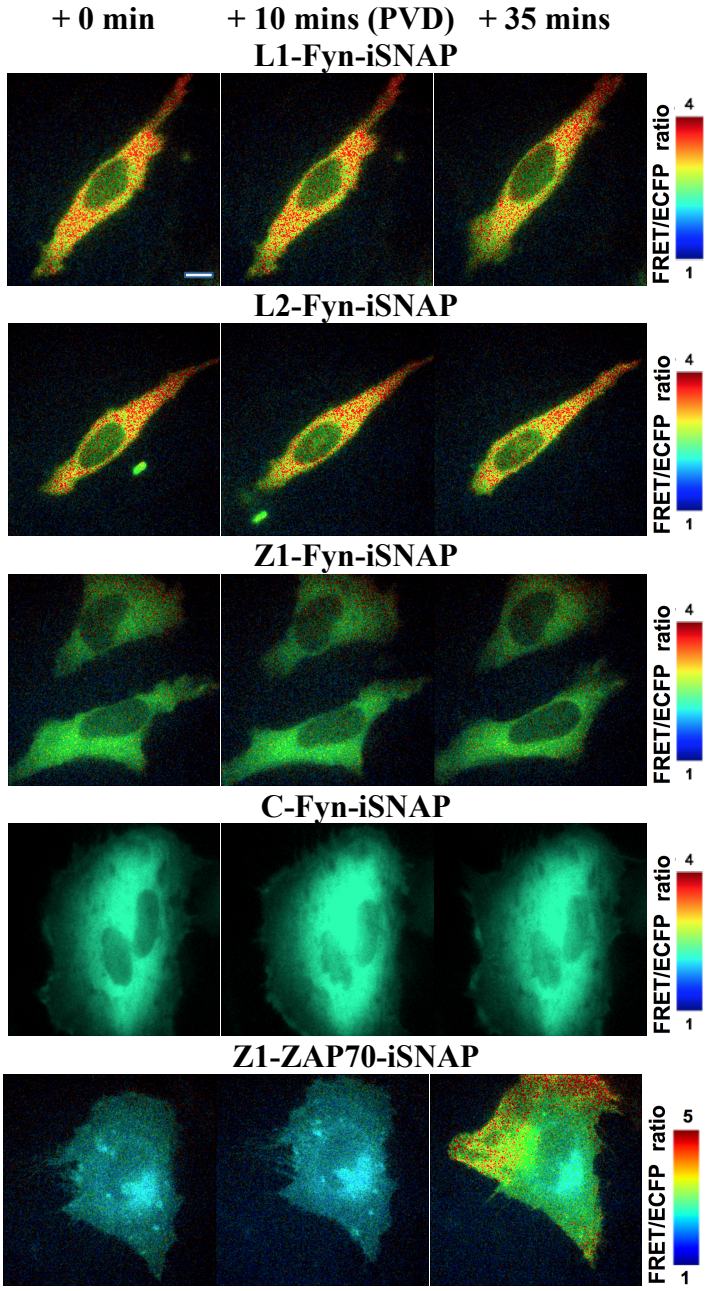

Figure 3: Time-lapse images of HeLa cells expressing Fyn-iSNAPs in response to PVD stimulation.These FRET/ECFP ratio images were subtracted by background, and they showed HeLa cells transfected with L1-Fyn-iSNAP, L2-Fyn-iSNAP, Z1-Fyn-iSNAP, C-Fyn-iSNAP and Z1-ZAP7-iSNAP (from top to bottom). The FRET/ECFP ratio in the images ranges from 1-5 for Z1-ZAP70-iSNAP and 1-4 for the rest of groups. Scale bar, 5 μm.

1.3 Discussion

In HeLa cells, all Fyn-iSNAPs showed no FRET/ECFP emission ratio change after PVD stimulation compared to their basal level. However, differences in their average FRET/ECFP ratio were observed in their original basal level. Since there is no tyrosine site at the N-terminus, C-Fyn-iSNAP served as a control construct that captured the FRET/ECFP ratio level when the ligand was not phosphorylated within the Fyn-iSNAPs. For Z1, which is a low-affinity binding partner of the Fyn SH2 domain but high-affinity binding partner of the ZAP70 SH2 domains, its Fyn-iSNAP and ZAP70-iSNAP showed a FRET/ECFP ratio basal level that was comparable to the negative control group. After PVD treatment, Z1-Fyn-iSNAP showed no change, but Z1-ZAP70-iSNAP showed significant change in the emission ratio. Thus, these results may indicate that only after PVD stimulation, the tyrosine sites on Z1 were phosphorylated so that there was a conformational change in Z1-ZAP70-iSNAP. However, since phosphorylated Z1 had low binding affinity to the Fyn SH2 domain, it may not be able to compete with regulatory $pTyr^{531}$ at C-terminus and to bind to the SH2 domain, which led to no FRET/ECFP ratio change. For L1 and L2, which contain a high-affinity binding region to the Fyn SH2 domain, their Fyn-iSNAPs demonstrated relatively high FRET/ECFP ratio before and after PVD treatment compared to C-Fyn-iSNAPs, and the addition of PVD did not increase the ratio further. Therefore, it was likely that the ligand region of L1- and L2-Fyn-iSNAPs were easily phosphorylated within HeLa cells and bound to the SH2 domain by competing with $pTyr^{531}$ at all time, which could cause conformational changes and increased FRET occurrence even before PVD stimulation. Thus, PVD treatment could not elicit any FRET/ECFP ratio change since L1 and L2 were already

phosphorylated in the HeLa cells. Measuring the phosphorylation level of Fyn-iSNAPs before and after PVD stimulation can test this hypothesis. Also, adding a proline-rich peptide to the Fyn SH2 domain-binding partner did not cause any difference in FRET/ECFP ratio, which means the high-affinity binding partner was the most important region in determining the overall structure of L1- and L2-Fyn-iSNAPs and FRET/ECFP ratio.

As mentioned earlier, a difference in the values of FRET/ECFP ratio was observed for HeLa transfected with Fyn-iSNAPs with different ligand regions. This difference may also indicate the potential of finding a specific ligand that gets phosphorylated only after PVD stimulation and has high affinity of binding to the Fyn SH2 domain after phosphorylation. With that ligand, truncated human PD-1 fused Fyn-iSNAP would be able to rewire PD-1/PD-L1 pathway in T cells and contribute to immunotherapy for cancers.

1.4 Materials & Methods

1.4.1 DNA construction and plasmids

LacZ-Fyn-iSNAP was constructed first by using polymerase chain reaction (PCR) to obtain the necessary DNA components, which were LacZ, ECFP-YPet FRET pair, human Fyn (Figure 1B). The components were assembled into pCBI vector through Gibson Assembly (New England Biolabs).

The LacZ region was replaced by various ligands of Fyn SH domains using Golden Gate Assembly (New England Biolabs). The ligand, L1, was EPQYEEIPIYL, which contained high-affinity binding partner of Fyn SH2 domain after phosphorylation [24]. The sequence of the second ligand, L2, was HSIAGPPVPPREPQYEEIPIYL, which had a proline-rich region and the same binding partner as in L1. ITAM region of CD3ζ-chains of TCR, NQLYNELNLGRREEYDVLDK, constitutes the third ligand for the SH2 domain of Fyn. All plasmids were purified with the QIAquick Gel Extraction Kit (Qiagen) and Miniprep Kit (Qiagen).

1.4.2 Cell culture and reagents

HeLa cells were obtained from American Tissue Culture Collection (ATCC) (Manassas, VA), and they were cultured in medium containing Dulbecco's modified Eagle medium (DMEM) (Gibco), 10% fetal bovine serum (FBS) (Atlanta Biologicals, Lawrenceville, GA), 1x GlutaMAX (Thermo Fisher) and 1x penicillin/streptomycin (Invitrogen). They were cultured in 37°C humidified-incubator with 5% CO_2. HeLa cells were transfected with the plasmids using Lipofectamine 3000 kit (Sigma-Aldrich) 48 hours before imaging. Cell starvation started 24 hours before imaging by culturing cell

with starvation medium containing advanced DMEM (Gibco), 1x GlutaMAX and 1x penicillin/streptomycin.

1.4.3 Image acquisition and analysis

Before imaging, the cells were plated onto glass-bottom dishes (Cell E&G) coated with fibronectin (Sigma) at 10 μg/mL concentration, and the coated dishes were kept at 37°C for 4 hours before cell plating. During imaging, the plated HeLa cells were maintained in the starvation medium at 37°C with CO_2 supplemented. The images recording the basal level of the cells were taken for at least 10 minutes. Then, cells were stimulated with pervanadate, which inhibited phosphatase activity within the cells and led to phosphorylation at the ligand region of the Fyn-iSNAP.

The images were collected with a Nikon eclipse Ti inverted microscope with 100x DIC Nikon microscope objective (NA 1.4) used and the MetaMorph 7.8.8.0 software (Molecular Devices). Furthermore, the microscope was installed with a 450DRLP dichroic mirror, a 420DF20 excitation filter, 475DF40 filter for ECFP and 535DF25 filter for YPet (Chroma).

Image analysis was conducted on Fluocell, which is an image analysis software developed at the Wang lab (data not published yet). The fluorescence intensity of non-transfected HeLa cells was set as the background, which is subtracted from the fluorescence signals of the transfected cells. Then, the pixel-by-pixel ratio images of FRET/ECFP were displayed in the intensity modified display (IMD) mode. For each pixel, the color was determined by the ECFP/FRET ratio, and ECFP fluorescence intensity determined the brightness.

Chapter 2: The reprogramming of SIRPα/CD47 inhibitory pathway in macrophage with SIRPα-iSNAPs

2.1 Background

2.1.1 The role of Fcγ receptors in macrophages

Macrophages are innate immune cells that are capable of eliminating cell debris and pathogens by phagocytosis, and this effector function is regulated by a complex mechanism involves balance between activating and inhibitory signals. Fcγ receptors (FcγRs) are expressed on the surface of macrophages, and they have binding specificity towards Fc domain of antibodies, which allows macrophages to bind to infected cells or pathogens [25]. This binding is important for the initiation of antibody-dependent cellular phagocytosis (ADCP) [26]. FcγRs have an immunoreceptor tyrosine-based activation motif (ITAM) in their cytoplasmic domain, and ligation of Fc domain to activating FcγR leads to the phosphorylation of ITAM region, which recruits Spleen tyrosine kinase (Syk) [27]. Syk phosphorylates and activates downstream molecules, such as PI3K and MAP kinase, which leads to an increase in cellular calcium level and eventually promotes phagocytosis [28]. Therefore, after monoclonal antibodies (mAbs) against tumor antigens were found, such as rituximab and cetuximab, macrophages were capable of engulfing and degrading targeted cancer cells in vitro [29].

2.1.2 The role of SIRPα receptor in macrophages

Besides pro-phagocytic signals from activating Fcγ receptors, phagocytosis is also regulated by inhibitory surface receptors, such as signal regulatory protein α (SIRPα), which negatively regulates the effector function of macrophage. The cytoplasmic domain of SIRPα contains inhibitory immunoreceptor tyrosine-based inhibition motifs (ITIMs)

[30]. When the extracellular domain of SIRPα interacts with a widely expressed transmembrane protein CD47, ITIMs get phosphorylated and bind to the SH2 domain of tyrosine phosphatase 1 (SHP1), which activates the phosphatase and initiates a signaling cascade that inhibits macrophage phagocytosis [31,32]. Thus, by interacting with inhibitory SIRPα receptor, CD47 serves as a "don't eat me" signal and a sign of "self", which is expressed on majority of normal tissue cells so that the cells will not be the targets of phagocytosis [33,34]. However, this CD47-SIRPα pathway is also utilized by cancers to evade the immune system by inhibiting macrophage phagocytosis. Upregulation of CD47 has been observed on multiple human tumor types, including acute and chronic myeloid leukemia, acute lymphoblastic leukemia, glioblastoma, hepatocellular carcinoma, ovarian and prostate tumor cells, and many others [35,36].

This evasion mechanism of utilizing the CD47-SIRPα pathway also offers the potential for treating cancers. Monoclonal antibodies directed against CD47 has been developed to inhibit the CD47-SIRPα pathway, which blocked the inhibitory signaling cascade and have shown tumor eradication of various cancer types in mouse xenotransplantation models [35,37,38]. However, hemolysis may occur during anti-CD47 cancer therapy since human red blood cells (RBCs) express high-level CD47 as well [39].

Therefore, rewiring CD47-SIRPα pathway in macrophages, combining with antibodies that specifically target tumor cells, offers a potential therapeutic strategy for cancer therapy with minimal off-target effects.

2.1.3 Shp2-iSNAP & Syk-iSNAP

In our previous study, an integrated sensing and activating protein (iSNAP) for macrophage phagocytosis was developed with either phosphatase Shp2 or kinase Syk as

the activating module, and these engineered proteins were used to replace the original SIRPα cytoplasmic domain (data not published yet). The tyrosine phosphatase Shp2 is autoinhibited, and its protein tyrosine phosphatase (PTP) domain is occluded by the N-SH2 domains [40]. Upon binding to a phosphorylated peptide, the N-SH2 domain moves away, which exposes the enzymatic domain and results in activated Shp2 [41]. The Shp2-iSNAP consists of a peptide containing tyrosine site (BTAM), ECFP and YPet fluorescent protein pair, and Shp2 without its C-terminal tail subsequently. ECFP and YPet can engage in fluorescence resonance energy transfer (FRET). Therefore, upon phosphorylation, the BTAM can bind to the N-SH2 domains, which allows ECFP and YPet to be in close proximity and leads to FRET/ECFP emission ratio changes. Also, when the N-SH2 domains bind to the BTAM, the PTP domain of Shp2 is simultaneously exposed, which leads to subsequent phosphatase activity. Therefore, upon CD47 engagement, SIRPα cytoplasmic domain is phosphorylated at the BTAM region within the engineered iSNAP, and instead of transducing anti-phagocytic signals through the phosphatase Shp1, SIRPα-Shp2-iSNAP senses phosphorylation at the BTAM region and simultaneously promotes macrophage pro-phagocytic Shp2 (data not published yet).

Based on the same principle as that of Shp2-iSNAP, Syk-iSNAP utilized Syk as the activating module with a sensing peptide derived from the ITAM motif of FcγRIIA and the same FRET pair. Instead of inhibiting macrophage phagocytosis via Shp1, the engineering SIRPα receptor with Syk-iSNAP promotes phagocytosis via the activation of Syk kinase (data not published yet).

For further research purposes, increasing gene delivery efficiency is needed. Preliminary experiments including the lentiviral infection of induced pluripotent stem

cells (iPSCs) demonstrated that the delivery of SIRPα-Shp2-iSNAP and SIRPα-Syk-iSNAP were not efficient due to their DNA sizes. Therefore, in order to characterize and utilize these engineered proteins in further applications, the sizes of the engineered SIRPα-Shp2-iSNAP and SIRPα-Syk-iSNAP were reduced in this study, and the truncated proteins were tested in macrophages to determine if they retain their original capability of rewiring SIRPα/CD47 pathway.

2.2 Results

2.2.1 Development and characterization of the size-reduced SIRPα-iSNAPs in mouse macrophages

The size-reduction of SIRPα-iSNAPs started with the removal of ECFP and YPet flurophore pair since the removal would potentially had no effects on the rewiring and activating functions of the engineered proteins. Thus, ECFP, YPet and the linker between them were removed from the original SIRPα-iSNAPs and replaced by flexible peptide linkers, such as 17mer, 34mer and EV linker [42,43]. 17mer linker is consisted of GSTSGSGKPGSGEGSTK, and 34mer linker has 34 amino acids that are consisted of two 17mer linkers [42]. EV linker has 116 amino acids [43]. In order to visualize the engineered cells using flow cytometry or imaging, YPet was added at the C-terminus of the truncated SIRPα-iSNAPs (Figure 4).

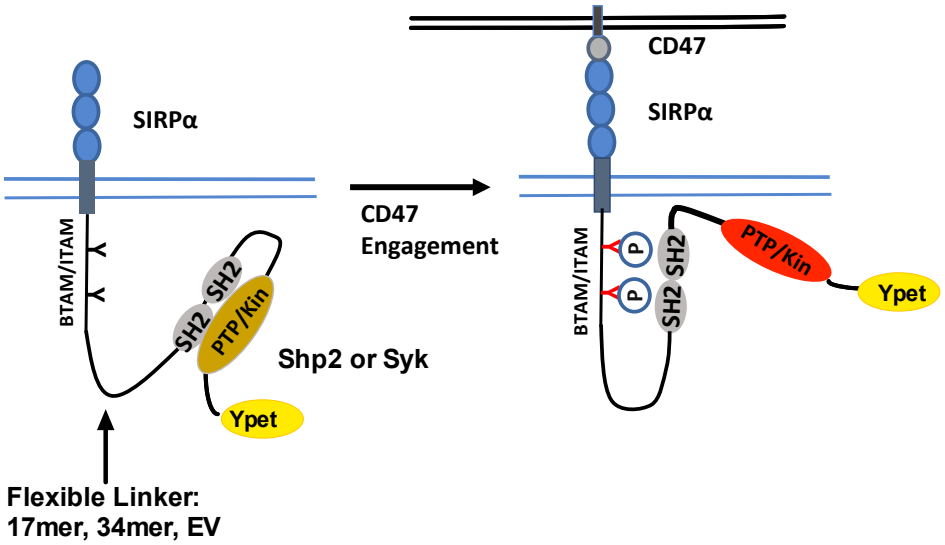

Figure 4: Schematic drawing of the truncated SIRPα-iSNAP and its intended activation mechanism upon CD47 engagement. Upon CD47 engagement, the BTAM/ITAM region gets phosphorylated, which leads to the autoinhibitory N-SH2 domains binding to this region. Then, the enzymatic domain within Shp2 or Syk will be exposed, which leads to Shp2/Syk activation and downstream activating signaling.

Functionality of the size-reduced iSNAPs was tested in RAW264.7 macrophages. After RBCs with high level of CD47 expression were stained with CellTracker™ Deep Red and opsonized with rabbit anti-hRBC IgG, they were incubated with the macrophages. Then, the engulfment efficiency was detected by using flow cytometer. As shown in Figure 5, SIRPα-Shp2-iSNAP-34mer, SIRPα-Shp2-iSNAP-EV and SIRPα-Syk-iSNAP-EV showed higher phagocytosis efficiency compared to the negative control group, which was the original full-length SIRPα receptor fused with YPet (SIRPα-FL-YPet). Since SIRPα-Shp2-iSNAP-17mer did not show a significant difference compared to negative control, this experimental group was excluded from subsequent experiments.

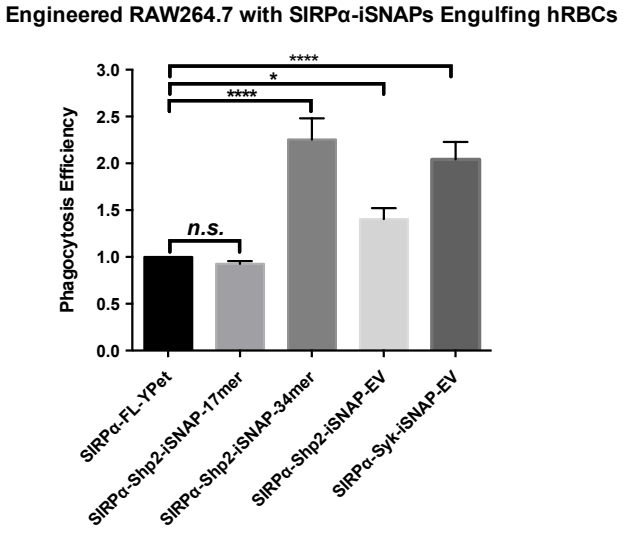

*Figure 5: The phagocytic efficiency of the size-reduced SIRPα-iSNAPs in RAW264.7. Bar graph (mean ± S.E.M.) of normalized phagocytic efficiency of RAW264.7 expressing the negative control group against opsonized RBCs. **** ($P < 0.0001$), * ($P < 0.05$) and n.s. ($P > 0.05$) are from ordinary one way ANOVA.*

2.2.2 Characterization of the SIRPα-iSNAPs and the size-reduced SIRPα-iSNAPs in human macrophages

At the same time, whether the iSNAP constructs can also enhance the phagocytosis of human promyelocytic leukemia cell derived macrophages (PLDMs) was examined using HL60. This was the first time that SIRPα-iSNAPs were confirmed to express correctly in human PLDMs. Also, by utilizing lentiviral infection and cell sorting, a robust and highly efficient approach was developed to obtain engineered macrophages from promyelocytic leukemia cells (Figure 6). Then, the phagocytic power of engineered PLDMs was tested against opsonized RBCs and non-opsonized RBCs (Figure 6). PLDMs with SIRPα-Shp2-iSNAP demonstrated increased phagocytosis efficiency against opsonized RBCs compared to native PLDMs and those with anti-phagocytic SIRPα-FL-YPet, but the PLDMs expressing SIRPα-Shp2-iSNAP did not have enhanced efficiency against non-opsonized RBCs. In addition, the phagocytic power of the engineered PLDMs against tumor cells was also tested. This experiment used Toledo, a human non-Hodgkin's lymphoma (NHL) cell line that expresses CD20. The engineered PLDMs with SIRPα-Shp2-iSNAP demonstrated increased engulfment of Toledo cells opsonized by anti-CD20 antibody (Figure 6C), and the putative mechanism was shown in Figure 7.

After development of the size-reduced SIRPα-Shp2-iSNAPs, they were transduced into HL60 as well. Following cell sorting procedure, HL60 cells expressing SIRPα-Shp2-iSNAP-34mer and SIRPα-Shp2-iSNAP-EV were enriched, which then were derived into engineered macrophages. Then, the phagocytic power of these engineered PLDMs was tested against opsonized RBCs, and the results were shown in Figure 8.

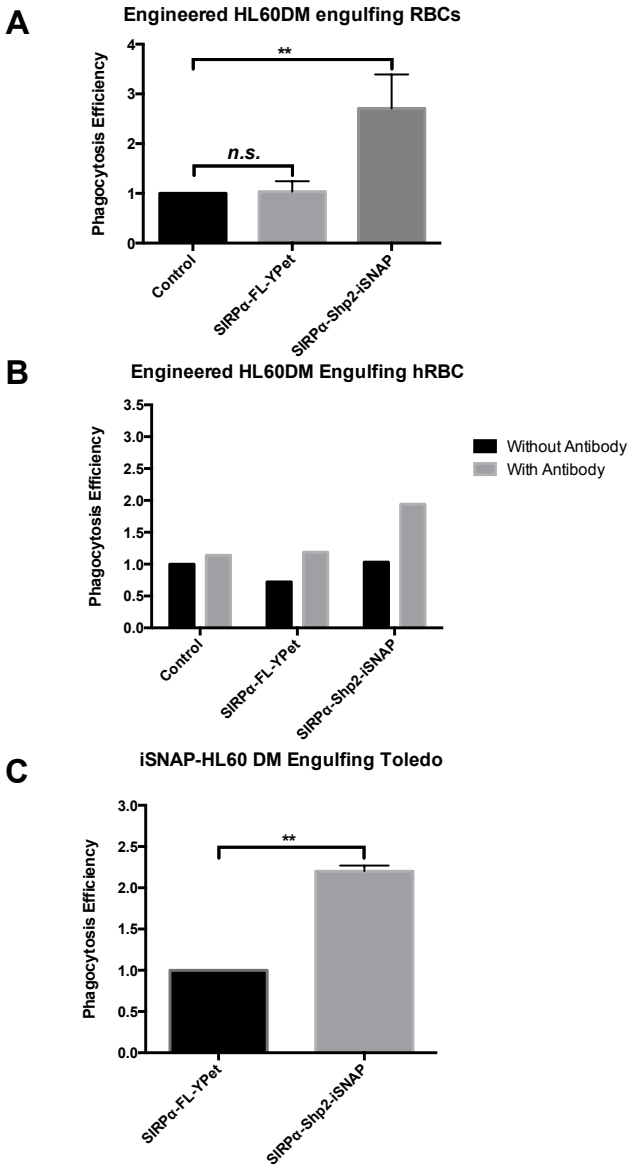

*Figure 6: The phagocytic efficiency of SIRPα-Shp2-iSNAPs in PLDMs. (A) Bar graph (mean ± S.E.M.) of normalized phagocytic efficiency of PLDMs expressing SIRPα-Shp2-iSNAP against opsonized human RBCs. ** ($P < 0.001$) and n.s. ($P > 0.05$) are from ordinary one way ANOVA. (B) The comparison of the phagocytosis efficiency of PLDMs against opsonized or non-opsonized RBCs. (C) Bar graph (mean ± S.E.M.) of normalized phagocytic efficiency of PLDMs expressing SIRPα-Shp2-iSNAP against rituximab-opsonized Toledo cells. ** ($P < 0.001$) is from two-tailed Student t-test.*

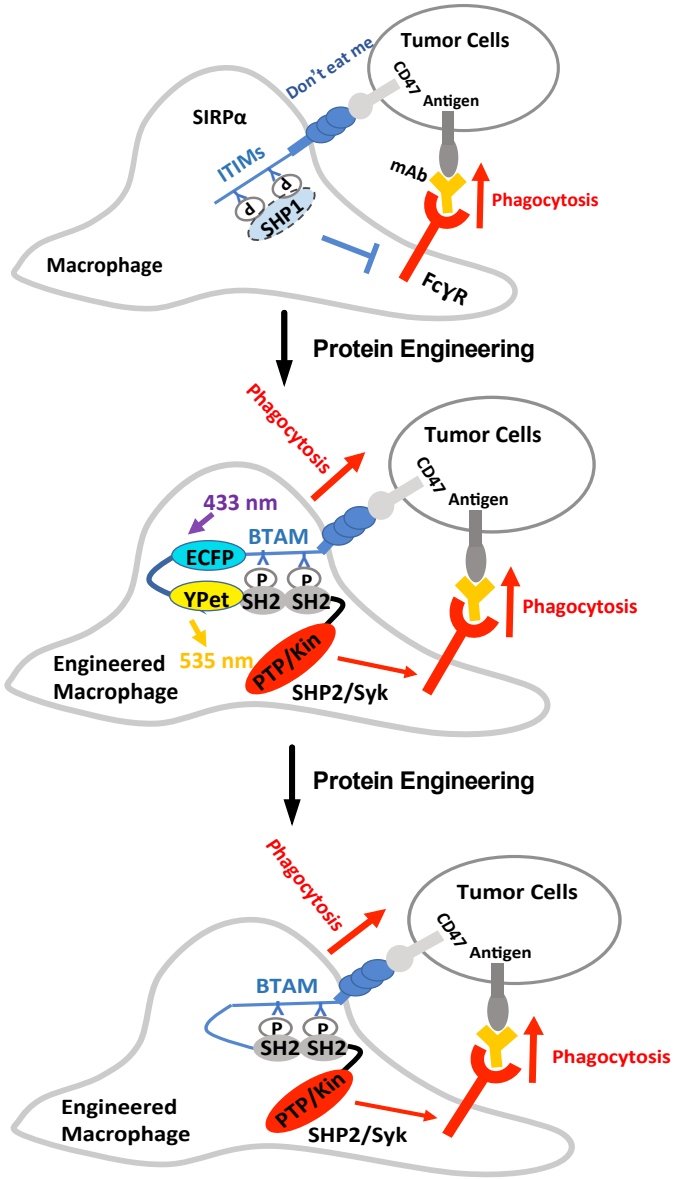

Figure 7: Schematic drawing of the engineered macrophage for antibody-mediated tumor cell phagocytosis. In native macrophages, upon CD47 ligation, PD-1 receptor transduces inhibitory signaling through SHP1, which inhibits FcγR. In previously engineered macrophages, SIRPα-iSNAPs not only further promote phagocytosis via Shp2/Syk kinase but also utilize FRET within iSNAP to simultaneously report the activation of the activating modules. At last, the truncated SIRPα-iSNAPs retain the activating function but not the monitoring function.

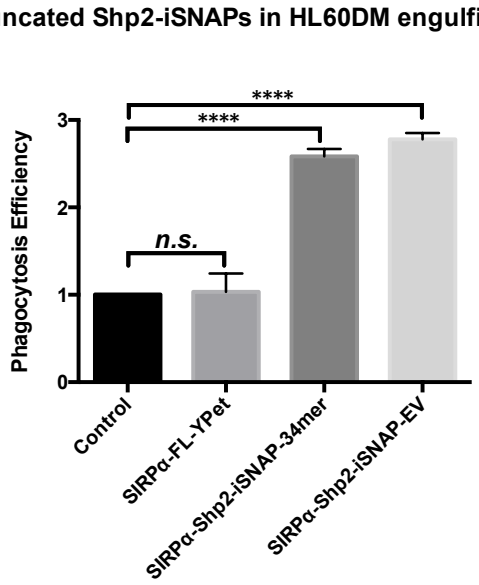

*Figure 8: The phagocytic efficiency of SIRPα-Shp2-iSNAPs in PLDMs. Bar graph (mean ± S.E.M.) of normalized phagocytic efficiency of PLDMs expressing the truncated SIRPα-Shp2-iSNAP against opsonized human RBCs. **** ($P < 0.0001$) and n.s. ($P > 0.05$) are from ordinary one way ANOVA.*

2.3 Discussion

The size-reduced SIRPα-Shp2-iSNAP demonstrated different levels of phagocytosis efficiency against RBCs in macrophages. This increased efficiency of the engineered macrophages with SIRPα-Shp2-iSNAP-34mer and SIRPα-Shp2-iSNAP-EV was consistent with the previous results of the original SIRPα-iSNAP-Shp2. However, SIRPα-Shp2-iSNAP-17mer did not show increased phagocytosis efficiency. The only difference among the constructs was the length of the linker between the tyrosine-containing BTAM region and Shp2. As mentioned earlier, the activation of iSNAP-Shp2 was relying on the autoinhibitory N-SH2 domains in Shp2 to bind to the BTAM and exposing the enzymatic PTP domain [24]. 17mer has the shortest linker length among all the linkers, and the data demonstrated that the phagocytic power of RAW264.7 transfected with SIRPα-Shp2-iSNAP-17mer was not increased, while those transfected with SIRPα-Shp2-iSNAP-34mer and SIRPα-Shp2-iSNAP-EV showed augmented phagocytosis. Therefore, the length of the linker played a role in the functionality of the size-reduced SIRPα-Shp2-iSNAP. With too short linker, the SH2 domains in Shp2 might not be able to bind to the BTAM due to structural hindrance, or the construct misfolded in the process so that the construct lost its function. For the first situation, the SH2 domains may still occlude the PTP domain, and Shp2 could not be activated properly, which may explain why the phagocytosis efficiency was not augmented for the macrophages transfected with SIRPα-Shp2-iSNAP-17mer. When the linker length was doubled by utilizing 34mer, the phagocytosis efficiency was increased significantly, and when the linker length became even longer, the efficiency decreased compared to 34mer but still significantly higher than the negative control group. This result indicated that the length

of the linker region influences the functionality of the SIRPα-Shp2-iSNAP constructs in macrophages, and an optimal length can be determined to maximize the functionality of this engineered protein and to successfully rewire the SIRPα-CD47 pathway.

The sized-reduced SIRPα-Shp2-iSNAP, such as SIRPα-Shp2-iSNAP-34mer and SIRPα-Shp2-iSNAP-EV, showed enhanced engulfment toward opsonized RBCs as well, which indicated that they retained the rewiring and activating functions of the original SIRPα-Shp2-iSNAP. Therefore, with their reduced sizes, the efficiency of their lentiviral production and infection will greatly increase, which allows iSNAPs to be easier to apply in future experiments.

The engulfment assay of the engineered PLDMs against opsonized RBCs and non-opsonized RBCs was also conducted. Overall, both the engineered PLDMs and the native PLDMs had increased phagocytosis of opsonized RBCs than that of non-opsonized RBCs. After opsonization, engineered PLDMs with SIRPα-Shp2-iSNAP demonstrated more engulfment of RBCs than the other control groups. For non-opsonized RBCs, SIRPα-Shp2-iSNAP did not show an elevated level of engulfment. By comparing the phagocytosis efficiency with and without antibody-opsonization, the results demonstrated that the macrophages expressing SIRPα-Shp2-iSNAP required antibody-mediation for their phagocytosis of CD47 expressing cells, which fulfill our goal of minimizing off-target effects for our engineered iSNAPs in immunotherapy.

In addition, the results also indicated that the engineering of SIRPα/CD47 pathway in human macrophages using SIRPα-Shp2-iSNAP can promote the antibody-mediated tumor cell phagocytosis. Therefore, engineered iSNAPs with activating module Shp2 or Syk are capable of reprograming inhibitory SIRPα/CD47 pathway. Even with

overexpression of CD47 in tumor cells, since iSNAPs can reprogram the original anti-phagocytic SIRPα/CD47 signaling into a pro-phagocytic one, CD47 ligation further promotes phagocytosis of engineered macrophages against those tumor cells. Thus, the engineered human macrophages with SIRPα-iSNAP working with mAbs that specifically target against tumor cells could lead to engulfment and eradication of tumor cells. At the same time, the function of mAbs could help minimize off-target effects against other CD47 expressing tissue cells.

2.4 Materials & Methods

2.4.1 Plasmid construction

The Shp2-iSNAP-LacZ was constructed first by using Gibson Assembly ((New England Biolabs) to fuse pSIN vector, SIRPα with BTAM instead of ITIM, LacZ, truncated human Shp2 and YPet together. Then by utilizing Golden Gate reaction relying on BsmBI sites in the construct, the LacZ region of Shp2-iSNAP-LacZ was replaced with 17mer, 34mer and EV linker to create Shp2-iSNAP-17mer, -34mer and -EV. The Syk-iSNAP-EV was constructed by fusing SIRPα without ITIM, ITAM region, EV linker, full-length Syk and YPet into pSIN vector using Gibson Assembly. The sequences of plasmids were verified by DNA sequencing.

2.4.2 Cells and reagents

RAW264.7, Toledo, HEK293T and HL60 were obtained from ATCC (Manassas, VA). RAW264.7 were maintained in medium containing DMEM (Gibco), 10% fetal bovine serum (FBS) (Atlanta Biologicals, Lawrenceville, GA), 1x GlutaMAX (Thermo Fisher) and 1 x penicillin/streptomycin (Invitrogen). Toledo and HL60 were grown in RPMI 1640 (Invitrogen, Carlsbad, CA), added with 10% FBS, 1x GlutaMAX and 1% penicillin/streptomycin. These cells were cultured in 37°C humidified-incubator supplemented with 95% air and 5% CO2.

2.4.3 RBC source

Human peripheral blood samples were provided by VA San Diego Medical Center, San Diego, CA with an IRB-approved protocol (VA San Diego IRB# H150008).

2.4.4 Lentivirus production

HEK293T cells were transfected with pSIN vector carrying SIRPa-iSNAPs, the packaging plasmid pSPAX2, and the envelope-encoding plasmid pMD.G by using Lipofectamine 2000 (Life technologies) [44]. After 72 hours culture, the media containing lentivirus were harvested and centrifuged at 1250 rpm for 5 minutes. Then, the supernatant was filtered through a 0.45 um syringe filter (Merck Millipore ltd.), and PEG-it^{TM} (System Biosciences) were added to precipitate the virus. The mixture was shaken at 4 °C overnight, which was centrifuged at 1500 g for 30 minutes the next day to obtain virus pellet. The pellet was suspended with DMEM medium for infection.

2.4.5 Electroporation of macrophages

SIRPa-iSNAPs were introduced into RAW 264.7 by electroporation. 3 x 10^6 RAW 264.7 were re-suspended in 220 µl of RPMI 1640 and added with 15 µg plasmids. Then the cell were electroporated in 4mm cuvette (Genesee Scientific Inc.) (250V, 950 mF, ∞ Ω), and they were cultured in 2 mL of DMEM with 10% FBS and 1 x GlutaMAX.

2.4.6 Monocytic differentiation

HL60 cells were transduced with concentrated lentivirus, and they were counted using a haemocytometer, and 1 x 10^6/ 3 mL cells were used in each 35 mm dishes (Thermo). Then, these cells are treated immediately with 20 ng/mL of 12-O-tetradecanoylphorbol-l3-acetate (PMA) (Sigma-Aldrich) for 72 hrs, and the differentiated macrophages were used for phagocytosis assay.

2.4.7 Phagocytosis assay

For phagocytosis assays, transfected macrophages were plated in 60 mm dishes (Thermo). RBCs and Toledo were washed twice PBS, and incubated with 1 μM and 0.3 μM CellTracker^{TM} Deep Red dye (Life technologies) respectively in PBS for an hour at 37°C. Then, extra dye was washed away by two times of wash with PBS plus 0.5% FBS, and the cells were resuspended in PBS plus 0.5% FBS.

RBCs were opsonized by rabbit anti-hRBC IgG (0.5 μg/ml) (Cambridge, USA), and Toledo cells were opsonized by rituximab (ImClone LLC.). Then, labeled and opsonized RBCs were incubated with RAW264.7 at a ratio of 10:1 for 30 minutes in the incubator. After incubation with the macrophage, RBCs that were not engulfed were removed by washing with PBS plus 0.5% FBS twice and lysed by adding ACK buffer (NH_4Cl 31 mM, $KHCO_3$ 2 mM, EDTA 20 μM) for 1 minute.

For Toledo cells, labeled cells and rituximab (10 μg/ml) were added together to PLDMs at a ratio of 10:1 and incubate at 37 °C for three hours. After incubation, Toledo cells that were not engulfed were removed by washing with PBS, and the removal efficacy was confirmed under microscope. At last, macrophages were detached by scratching the dish with cell lifters and kept in PBS with 0.5% FBS, which were read by flow cytometer for phagocytosis efficiency.

2.4.8 Flow cytometry

Engineered macrophages had YPet expression, which has excitation of 488 nm and emission of 575/26 nm. Thus, these cells were measured by flow cytometry and gated. Then, the signal of engulfed cells (Deep Red, Ex:640 nm, Em:660/20 nm) were measured among the engineered macrophage population, and the average signal intensity was calculated to determine the phagocytosis efficiency.

References

1. Palacios, Emil H., and Arthur Weiss. "Function of the Src-family kinases, Lck and Fyn, in T-cell development and activation." Oncogene 23.48 (2004): 7990.

2. Abraham, Robert T., and Arthur Weiss. "Jurkat T cells and development of the T-cell receptor signalling paradigm." *Nature reviews. Immunology* 4.4 (2004): 301.

3. Chan, A. C., Iwashima, M., Turck, C. W., & Weiss, A.. "ZAP-70: a 70 kd protein-tyrosine kinase that associates with the TCR ζ chain." Cell 71.4 (1992): 649-662.

4. Wang, H., Kadlecek, T. A., Au-Yeung, B. B., Goodfellow, H. E. S., Hsu, L. Y., Freedman, T. S., & Weiss, A.. "ZAP-70: an essential kinase in T-cell signaling." Cold Spring Harbor perspectives in biology 2.5 (2010): a002279.

5. Latchman, Y., Wood, C.R., Chernova, T., Chaudhary, D., Borde, M., Chernova, I., Iwai, Y., Long, A.J., Brown, J.A., Nunes, R. and Greenfield, E.A.. "PD-L2 is a second ligand for PD-1 and inhibits T cell activation." *Nature immunology* 2.3 (2001): 261-268.

6. Bennett, F., Luxenberg, D., Ling, V., Wang, I. M., Marquette, K., Lowe, D., ... & Collins, M.. "Program death-1 engagement upon TCR activation has distinct effects on costimulation and cytokine-driven proliferation: attenuation of ICOS, IL-4, and IL-21, but not CD28, IL-7, and IL-15 responses." *The Journal of Immunology* 170.2 (2003): 711-718.

7. Shinohara, T., Taniwaki, M., Ishida, Y., Kawaichi, M., & Honjo, T.. "Structure and chromosomal localization of the human PD-1 gene (PDCD1)." *Genomics* 23.3 (1994): 704-706.

8. Chemnitz, J. M., Parry, R. V., Nichols, K. E., June, C. H., & Riley, J. L.. "SHP-1 and SHP-2 associate with immunoreceptor tyrosine-based switch motif of programmed death 1 upon primary human T cell stimulation, but only receptor ligation prevents T cell activation." *The Journal of Immunology* 173.2 (2004): 945-954.

9. Chinai, J. M., Janakiram, M., Chen, F., Chen, W., Kaplan, M., & Zang, X.. "New immunotherapies targeting the PD-1 pathway." *Trends in pharmacological sciences* 36.9 (2015): 587-595.

10. Boussiotis, V. A., Chatterjee, P., & Li, L.. "Biochemical signaling of PD-1 on T cells and its functional implications." *Cancer journal (Sudbury, Mass.)* 20.4 (2014): 265.

11. Raab, M., Cai, Y. C., Bunnell, S. C., Heyeck, S. D., Berg, L. J., & Rudd, C. E.. "p56Lck and p59Fyn regulate CD28 binding to phosphatidylinositol 3-kinase, growth factor receptor-bound protein GRB-2, and T cell-specific protein-tyrosine kinase ITK: implications for T-cell costimulation." *Proceedings of the National Academy of Sciences* 92.19 (1995): 8891-8895.

12. Da Silva, A. J., Li, Z., De Vera, C., Canto, E., Findell, P., & Rudd, C. E.. "Cloning of a novel T-cell protein FYB that binds FYN and SH2-domain-containing leukocyte protein 76 and modulates interleukin 2 production." *Proceedings of the National Academy of Sciences* 94.14 (1997): 7493-7498.

13. Da Silva, A. J., Li, Z., De Vera, C., Canto, E., Findell, P., & Rudd, C. E.. "Tau interacts with src-family non-receptor tyrosine kinases." Journal of cell science 111.21 (1998): 3167-3177.

14. Sato, I., Obata, Y., Kasahara, K., Nakayama, Y., Fukumoto, Y., Yamasaki, T., Yokoyama, K.K., Saito, T. and Yamaguchi, N.. "Differential trafficking of Src, Lyn, Yes and Fyn is specified by the state of palmitoylation in the SH4 domain." *Journal of cell science* 122.7 (2009): 965-975.

15. Boggon, Titus J., and Michael J. Eck. "Structure and regulation of Src family kinases." *Oncogene* 23.48 (2004): 7918.

16. Schindler, T., Sicheri, F., Pico, A., Gazit, A., Levitzki, A., & Kuriyan, J.. "Crystal structure of Hck in complex with a Src family–selective tyrosine kinase inhibitor." *Molecular cell* 3.5 (1999): 639-648.

17. Sicheri, F., Moarefi, I., & Kuriyan J.. "Crystal structure of the Src family tyrosine kinase Hck." *Nature* 385.6617 (1997): 602.

18. Xu, W., Doshi, A., Lei, M., Eck, M. J., & Harrison, S. C.. "Crystal structures of c-Src reveal features of its autoinhibitory mechanism." *Molecular cell* 3.5 (1999): 629-638.

19. Ladbury, J. E., Hensmann, M., Panayotou, G., & Campbell, I. D.. "Alternative modes of tyrosyl phosphopeptide binding to a Src family SH2 domain: implications for regulation of tyrosine kinase activity." *Biochemistry* 35.34 (1996): 11062-11069.

20. Courtneidge, S. A., Goutebroze, L., Cartwright, A., Heber, A., Scherneck, S., & Feunteun, J.. "Identification and characterization of the hamster polyomavirus middle T antigen." *Journal of virology* 65.6 (1991): 3301-3308.

21. Love, P. E., & Hayes, S. M.. "ITAM-mediated signaling by the T-cell antigen receptor." Cold Spring Harbor perspectives in biology 2.6 (2010): a002485.

22. Wang, Y., Shyy, J. Y. J., & Chien, S.. "Fluorescence proteins, live-cell imaging, and mechanobiology: seeing is believing." *Annu. Rev. Biomed. Eng.* 10 (2008): 1-38.

23. Huyer, G., Liu, S., Kelly, J., Moffat, J., Payette, P., Kennedy, B., Tsaprailis, G., Gresser, M.J. and Ramachandran, C.. "Mechanism of inhibition of protein-tyrosine phosphatases by vanadate and pervanadate." *Journal of Biological Chemistry* 272.2 (1997): 843-851.

24. Waksman, G., Shoelson, S. E., Pant, N., Cowburn, D., & Kuriyan, J.. "Binding of a high affinity phosphotyrosyl peptide to the Src SH2 domain: crystal structures of the complexed and peptide-free forms." *Cell* 72.5 (1993): 779-790.

25. Waksman, G., Shoelson, S. E., Pant, N., Cowburn, D., & Kuriyan, J.. "The function of Fc [gamma] receptors in dendritic cells and macrophages." *Nature Reviews Immunology* 14.2 (2014): 94-108.

26. Weiskopf, K., & Weissman, I. L.. "Macrophages are critical effectors of antibody therapies for cancer." *MAbs*. Vol. 7. No. 2. Taylor & Francis, 2015.

27. Nimmerjahn, F., & Ravetch, J. V.. "Fcγ receptors as regulators of immune responses." *Nature Reviews Immunology* 8.1 (2008): 34-47.

28. Crowley, M.T., Costello, P.S., Fitzer-Attas, C.J., Turner, M., Meng, F., Lowell, C., Tybulewicz, V.L. and DeFranco, A.L.. "A critical role for Syk in signal transduction and phagocytosis mediated by Fcγ receptors on macrophages." *Journal of Experimental Medicine* 186.7 (1997): 1027-1039.

29. Weiskopf, K., & Weissman, I. L.. "Macrophages are critical effectors of antibody therapies for cancer." *MAbs*. Vol. 7. No. 2. Taylor & Francis, 2015.

30. Barclay, A. N., & Brown, M. H.. "The SIRP family of receptors and immune regulation." *Nature reviews. Immunology* 6.6 (2006): 457.

31. Okazawa, H., Motegi, S.I., Ohyama, N., Ohnishi, H., Tomizawa, T., Kaneko, Y., Oldenborg, P.A., Ishikawa, O. and Matozaki, T.. "Negative regulation of phagocytosis in macrophages by the CD47-SHPS-1 system." *The Journal of Immunology* 174.4 (2005): 2004-2011.

32. Barclay, A. N., & Brown, M. H.. "The SIRP family of receptors and immune regulation." *Nature reviews. Immunology* 6.6 (2006): 457.

33. Gardai, S.J., McPhillips, K.A., Frasch, S.C., Janssen, W.J., Starefeldt, A., Murphy-Ullrich, J.E., Bratton, D.L., Oldenborg, P.A., Michalak, M. and Henson, P.M.. "Cell-surface calreticulin initiates clearance of viable or apoptotic cells through trans-activation of LRP on the phagocyte." *Cell* 123.2 (2005): 321-334.

34. Reinhold, M. I., Lindberg, F. P., Plas, D., Reynolds, S., Peters, M. G., & Brown, E. J.. "In vivo expression of alternatively spliced forms of integrin-associated protein (CD47)." *Journal of cell science* 108.11 (1995): 3419-3425.

35. Chao, M. P., Weissman, I. L., & Majeti, R.. "The CD47–SIRPα pathway in cancer immune evasion and potential therapeutic implications." *Current opinion in immunology* 24.2 (2012): 225-232.

36. Willingham, S.B., Volkmer, J.P., Gentles, A.J., Sahoo, D., Dalerba, P., Mitra, S.S., Wang, J., Contreras-Trujillo, H., Martin, R., Cohen, J.D. and Lovelace, P.. "The CD47-signal regulatory protein alpha (SIRPa) interaction is a therapeutic target for human solid tumors." *Proceedings of the National Academy of Sciences* 109.17 (2012): 6662-6667.

37. Chao, M.P., Alizadeh, A.A., Tang, C., Myklebust, J.H., Varghese, B., Gill, S., Jan, M., Cha, A.C., Chan, C.K., Tan, B.T. and Park, C.Y.. "Anti-CD47 antibody synergizes with rituximab to promote phagocytosis and eradicate non-Hodgkin lymphoma." *Cell* 142.5 (2010): 699-713.

38. Majeti, R., Chao, M.P., Alizadeh, A.A., Pang, W.W., Jaiswal, S., Gibbs, K.D., van Rooijen, N. and Weissman, I.L.. "CD47 is an adverse prognostic factor and therapeutic antibody target on human acute myeloid leukemia stem cells." *Cell* 138.2 (2009): 286-299.

39. Liu, J., Wang, L., Zhao, F., Tseng, S., Narayanan, C., Shura, L., Willingham, S., Howard, M., Prohaska, S., Volkmer, J. and Chao, M.. "Pre-clinical development of a humanized anti-CD47 antibody with anti-cancer therapeutic potential." *PloS one* 10.9 (2015): e0137345.

40. Weiss, A., & Schlessinger, J.. "Switching signals on or off by receptor dimerization." *Cell* 94.3 (1998): 277-280.

41. Tonks, N. K. "Protein tyrosine phosphatases: from genes, to function, to disease." *Nature reviews. Molecular cell biology* 7.11 (2006): 833.

42. Lei, L., Lu, S., Wang, Y., Kim, T., Mehta, D., & Wang, Y. . "The role of mechanical tension on lipid raft dependent PDGF-induced TRPC6 activation." *Biomaterials* 35.9 (2014): 2868-2877.

43. Komatsu, N., Aoki, K., Yamada, M., Yukinaga, H., Fujita, Y., Kamioka, Y., & Matsuda, M.. "Development of an optimized backbone of FRET biosensors for kinases and GTPases." *Molecular biology of the cell* 22.23 (2011): 4647-4656.

44. Lee, M. H., Padmashali, R., & Andreadis, S. T. "JNK1 is required for lentivirus entry and gene transfer." *Journal of virology* 85.6 (2011): 2657-2665.